We are IntechOpen, the world's leading publisher of Open Access books
Built by scientists, for scientists

4,800
Open access books available

122,000
International authors and editors

135M
Downloads

Our authors are among the

154
Countries delivered to

TOP 1%
most cited scientists

12.2%
Contributors from top 500 universities

CLARIVATE ANALYTICS
BOOK CITATION INDEX
INDEXED

WEB OF SCIENCE™

Selection of our books indexed in the Book Citation Index in Web of Science™ Core Collection (BKCI)

Interested in publishing with us?
Contact book.department@intechopen.com

Numbers displayed above are based on latest data collected.
For more information visit www.intechopen.com

Chapter 8

Fracture Toughness Determination with the Use of Miniaturized Specimens

Jan Dzugan, Pavel Konopik and Martin Rund

Additional information is available at the end of the chapter

http://dx.doi.org/10.5772/intechopen.73093

Abstract

Fracture mechanics has been used for decades nowadays, and methods have been well established in the community especially for standard-sized specimens. As it was mainly developed for large structure assessment against the brittle failure, standardized specimens are of large size at present. However, in many cases, these standard specimens are not possible to apply due to size requirements of the available experimental material or the size of the component considered. These can be cases of residual service life assessment of in-service components, local properties determination (e.g., across weld), anisotropy determination and assessment of mechanical properties of newly developed materials under laboratory conditions (e.g., SPD processed materials, etc.). Therefore, development of new methods using significantly smaller specimens has to be carried out, and procedures using smaller-sized specimens together with their validity limits and relation to standardly obtained results have to be provided in order to provide solution for wide applications.

Keywords: fracture mechanics, ductile fracture, brittle fracture, miniature specimens, local properties, anisotropy assessment

1. Introduction

Fracture toughness properties yield very essential information on the material behavior with the presence of the sharp crack. This information is in many cases crucial for design or decision about the further use or discarding the component from service. However in many such important cases, there is shortage of the experimental material, and thus assessment has to be done based on miniaturized specimen testing. Examples of the cases when shortage of the

IntechOpen

© 2018 The Author(s). Licensee IntechOpen. This chapter is distributed under the terms of the Creative Commons Attribution License (http://creativecommons.org/licenses/by/3.0), which permits unrestricted use, distribution, and reproduction in any medium, provided the original work is properly cited. CC BY

experimental material is only available can be residual service life assessment of in-service components, when the experimental material only by semi-destructive approach can be obtained. Cases during development of new materials, generally preparation of the materials with limited volume such as severe plastic deformation processes for bulk nanomaterials preparation. Recently, also for the assessment of the parts produced by additive manufacturing techniques are application for small-size specimen testing.

This chapter is going to provide overview of reporting values of the results obtained with the use of miniaturized specimens with hints how can be small-size-based results related to the standard-sized specimen results. These techniques enable assessment of the fracture behavior from small material volumes allowing, for example, also local anisotropy assessment. In the first part of the chapter, some theoretical background for small-size specimen testing is provided for different fracture regime behaviors ranging from brittle up to full ductile behavior. Several mini specimens' geometries are demonstrated here that are subsequently applied on the experimental materials. Three materials are presented here, ferritic steel used for Master Curve-based assessment and then stainless steel and Ti-alloy produced by additive manufacturing technology. The results are summarized in order to provide inside into the facture behavior assessment with the use of miniaturized specimens providing background for practical application of these approaches.

2. Specimen size and geometry influence on fracture toughness parameters

The effect of the specimen size and the geometry is variable with the material fracture behavior. Most of the technical materials exhibit transition behavior, and thus three basic regions can be distinguished: the lower shelf, transition and upper shelf.

Holzmann and Vlach [1, 2] suggested schematic diagram of fracture toughness behavior with temperature (see **Figure 1**), where following fracture toughness parameters are used for an analysis of the fracture behavior:

$K_{J0.2}$—fracture toughness after 0.2 mm of blunting and crack extension.

K_{Jm}—value of K_J at the maximum load F_{max} for stable fracture behavior and nonlinear test record.

K_{Ju}—post-ductile tearing cleavage fracture toughness; only J_c-tests terminated by cleavage prior to attaining the maximum load F_{max} were taken into account.

K_{JC}—fracture toughness for the onset of cleavage fracture after elastic-plastic deformation, but with no prior ductile tearing.

K_C—the fracture toughness at the onset of brittle fracture; test record linear or with no significant deviation from linearity, but size validity requirements of ASTM E399 are not met.

K_{IC}—plane strain fracture toughness.

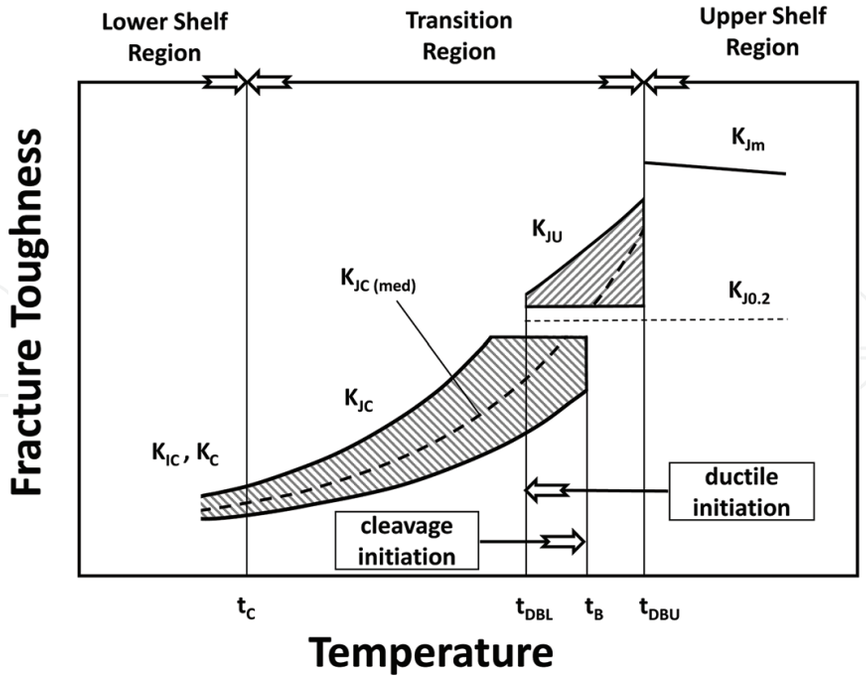

Figure 1. Schematic representation of fracture toughness-temperature dependence.

All values of K_J could be obtained by conversion from J-values using Eq. (1):

$$K_J = \sqrt{\frac{J.E}{(1-\nu^2)}} \tag{1}$$

The following transition temperatures are denoted in the diagrams:

t_{DBU}—ductile-brittle upper; the cleavage fracture occurs after certain amount of ductile tearing but prior to attaining the maximum load (the onset of the transition region).

t_{DBL}—ductile-brittle lower; the end of the region with the above fracture mode.

t_B—brittle-fracture transition temperature; the onset of the region, where cleavage fracture is initiated ahead of the blunted crack tip but without prior ductile tearing. Due to inherent scatter of material properties, t_B could be within the (t_{DBL}-t_{DBU}) region.

t_C—the lower shelf fracture toughness regime is below this temperature.

2.1. Brittle region (lower shelf region)

When a material behaves in a linear elastic manner prior to failure, such that the plastic zone is small compared to the specimen dimensions, a critical value of the Mode I stress intensity factor K_{Ic} may be an appropriate fracture parameter. In the ASTM E 399 [3] and similar test methods, K_{Ic} is referred to as "plane strain fracture toughness." Four specimen configurations are permitted for the fracture toughness determination by the current version of E 399: the compact tension (CT), single edge-notched bend bar (SE(B)), arc-shaped and disc-shaped specimens. However,

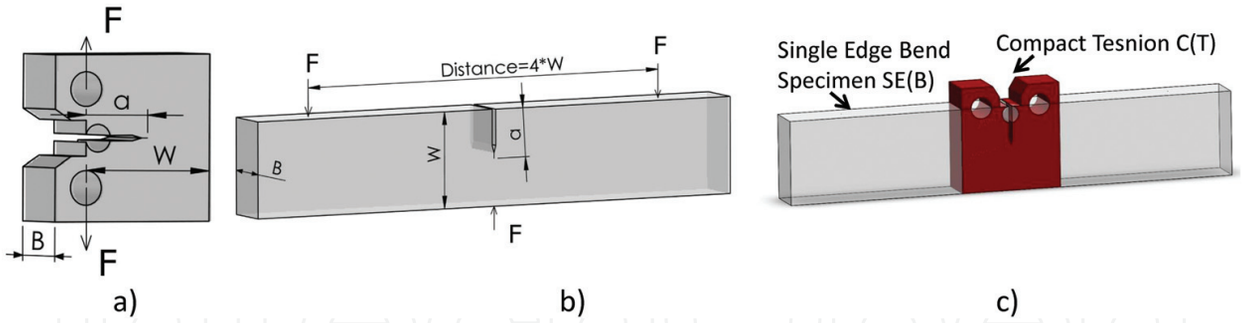

Figure 2. Comparison of the profiles of CT and SE(B) specimens with the same in-plane characteristic dimensions (*B, W, a*).

the vast majority of fracture toughness tests are performed on either CT or SE(B) specimens. **Figure 2** shows basic dimensions of both types of specimens of these two specimen types, assuming the same characteristic dimensions (*B, W, a*). It can be seen that the specimen design is such that all of the key dimensions (i.e., a, *B* and $W - a$) are approximately equal and, thus, geometry selection is only question of less material consumption from semi-product.

In order to fulfill the size requirements for size-independent fracture toughness value determination according to the ASTM E399, the minimal specimen thickness is 1.6 mm, while the specimen ligament size (*W-a*) must be not less than $2.5(K_{Ic}/\sigma_{YS})^2$, where σ_{YS} is the 0.2% offset yield strength. Considering recommended proportion of the thickness *B* which is nominally one-half the specimen width *W* and crack length, *a*, is nominally between 0.45 and 0.55 times the width *W*, the thickness must be also not less than $2.5(K_{Ic}/\sigma_{YS})^2$. These limits could be expressed using Eq. (2), which is not literally listed in the standard ASTM E399 but is noted in Anderson [4]:

$$B, a, (W-a) \geq 2,5 \cdot \left(\frac{K_{\mathrm{IC}}}{\sigma_{YS}}\right)^2 \; 0.45 \leq a/W \leq 0.55 \tag{2}$$

Because the size requirements of ASTM E 399 are very stringent, it is very difficult and sometimes impossible to measure a valid K_{Ic} for most of the structural materials. As an example, we can consider structural steel with σ_{YS} = 330 MPa and typical K_{Ic} values of 210 MPa.m$^{0.5}$. According to Eq. (2), the required thickness must be higher than 1 m, and the width (since $a/W = 0.5$) must be more than 2 m (see **Table 1**). Materials are seldom available in such dimensions, and if yes, machining and testing would have to be done using special machine, and all investigation would be extremely expensive. On the other hand, material such as tool steels exhibits high yield strength and low fracture toughness, and **Table 1** shows combination of these two values for obtaining valid fracture toughness value under plain

Example	σ_{YS}	K_{Ic}	B, a	B, a
	MPa	MPa.m$^{0.5}$	m	mm
Steel_1	330	210	1012	1012.4
Steel_2	1600	40	0.002	1.6

Table 1. Examples of the calculated thickness *B* for given σ_{YS} and K_{Ic} values.

strain condition for thickness 1.6 mm. Considering investigated material in this chapter, **Table 2** shows hypothetic K_{Ic} value under plain strain condition for different specimen geometries and sizes. Note that the toughness level calculated here corresponds to the lower shelf for these materials. Thus valid K_{Ic} tests on these materials would be possible only at low temperatures, where the materials are too brittle for most structural applications.

In ASTM E 399 it is listed that "Variation in the value of K_{Ic} can be expected within the allowable range of specimen proportions, a/W and W/B. K_{Ic} may also be expected to rise with increasing ligament size. Notwithstanding these variations, however, K_{Ic} is believed to represent a lower limiting value of fracture toughness (for 2 % apparent crack extension) in the environment and at the speed and temperature of the test."

Therefore, valid K_{Ic} is generally accepted as size-independent value though some minor deviation could not be avoided. As it can be seen from **Tables 1** and **2**, it is very difficult to obtain valid fracture toughness values with the use of subsized specimens in this region, except for very brittle materials. Therefore, subsided specimens will most yield size-dependent values of the fracture toughness.

2.2. Ductile-brittle transition region

In this region, micro-mechanisms of cleavage fracture cause that the cleavage toughness data tend to be highly scattered when compared to the lower shelf region, and thus a statistical analysis must be performed as shown in **Table 3**. Rather than single value of toughness at a particular temperature, the material has a toughness distribution. Research over the past three decades on the fracture of ferritic steels in the ductile-brittle transition region has led to two important conclusions:

Material	Specimen geometry and size	σ_{YS}	B, a	Requested K_{Ic}
		MPa	mm	MPa.m$^{0.5}$
15CH2NMFA	1 T-CT	502	25.0	50.2
	M-CT		4.0	20.1
	CVN 10 × 10 × 55		10.0	31.7
	KLST 4 × 2 × 27		2.0	14.2
AISI 304	1 T-CT	657	25.0	65.7
	M-CT		4.0	26.3
	CVN 10 × 10 × 55		10.0	41.6
	KLST 4 × 2 × 27		2.0	18.6
AM Ti6Al4V	1 T-CT	927	25.0	92.7
	M-CT		4.0	37.1
	CVN 10 × 10 × 55		10.0	58.6
	KLST 4 × 2 × 27		2.0	26.2

Table 2. Calculated requested parameter K_{Ic} for valid plain strain condition considering investigated material in this chapter.

Material	Tests							Region of fracture toughness results
	Tensile tests		Facture toughness tests					
	Standard	Mini	1 T-CT	0.16 T-CT	CVN	KLST	2 T-CT	
15CH2NMFA	X	X	X	X	X	X	X	Transition region
AISI 304	X	X	X	X	X	X		Upper shelf
Ti6AL4V		X		X	X			Upper shelf

Note: CVN, standard Charpy V-notched specimen ($10 \times 10 \times 55$ mm^3).

Table 3. Test matrix for the fracture toughness tests.

1. Scatter in fracture toughness data in the transition region follows a characteristic statistical distribution that is very similar for all ferritic steels.
2. The shape of the fracture toughness vs. temperature curve in the transition range is virtually identical for all ferritic steels. The only difference between steels is the absolute position of this curve on the temperature axis.

ASTM E1921 [5] implements this knowledge, and the standard outlines a fracture toughness test method that is based on the Master Curve concept for ferritic steels with yield strengths ranging from 275 to 825 MPa. Thanks to previous research, methodology for determination of toughness distribution is greatly simplified including size effect prediction. In order to directly compare toughness data obtained from different thickness specimens, a statistical size correction is employed to equilibrate the highly stressed material volume sampled at the crack tip by cleavage. The following Eq. (3), derived from ASTM E1921, shall be used for conversion to an equivalent value of $K_{Jc(1T)}$ for a reference 1 T specimen with thickness of $B_{1T} = 25$ mm:

$$K_{Jc(1T)} = 20 + \left(K_{Jc(X)} - 20\right).\left(\frac{B_X}{B_{1T}}\right)^{1/4} \tag{3}$$

where $K_{Jc(X)}$ is measured fracture toughness of the tested specimen and Bx refers to the nominal thickness of the tested specimen in millimeters, regardless of side grooves. Once toughness values at a fixed temperature have been converted to 1 T equivalent values, the further evaluation which leads to a reference transition temperature T_0 is performed according to standard as for 1 T specimen.

The reference temperature T_0 should be relatively independent of the test temperature that has been selected. Hence, data that are distributed over a restricted temperature range, namely, $T_0 \pm 50°C$, can be used to determine T_0. This temperature range together with the specimen size requirement (see Eq. (4)) provides a validity window for application of the Master Curve methodology. As an example, such a validity window for Charpy-size fracture specimens (W = B = 10 mm, a/W = 0.5) is shown in **Figure 3**.

$$K_{JC(\mathrm{lim}it)} = \sqrt{\frac{Eb_0\sigma_{ys}}{30.(1-\nu^2)}} \tag{4}$$

where E is the Young's modulus, σ_{ys} is the material yield strength at the test temperature and b_0 is ligament W-a.

It should be also mentioned that specimens can have side grooves, but they are optional (see **Figure 4**). In fact, side grooving may be indispensable as a means for controlling crack front straightness in bend bars of square cross section. The total side-grooved depth shall not exceed 0.25B. Side grooves with an included angle of 45° and a root radius of 0.5 ± 0.2 mm usually produce the desired results.

In the ASTM E1921 is noted that at high values of fracture toughness relative to specimen size and material flow properties, the values of K_{Jc} that meet the requirements of Eq. (3) may not always provide a unique description of the crack front stress strain fields due to some loss of constraint caused by excessive plastic flow. The application which played a key role for development of small specimen test technology (SSTT) was the evaluation of properties of irradiated materials. For example, many investigations for integrity assessments of nuclear components were done in VTT in Finland where also Master Curve method was developed [7] and validated [8]. Wallin et al. were further developing SSTT for Master Curve determination using mini-Charpy specimen (KLST) since 1997 [9]. Scibetta et al. [10] investigated different reactor pressure vessel steels using standard and miniature specimens. The reference temperatures obtained from subsize SE(B) and C(T) geometry tend to give a lower reference temperature by about −8.5°C than larger specimens which was considered as a consequence of the constraint loss. Kima et al. [11] investigated effects of specimen size on fracture toughness using 1 CT, 1/2 CT and 1/4 CT. It was found that small specimen test technique for F82H steel can be applicable to evaluate the fracture toughness properties due to no substantial effects of specimen size.

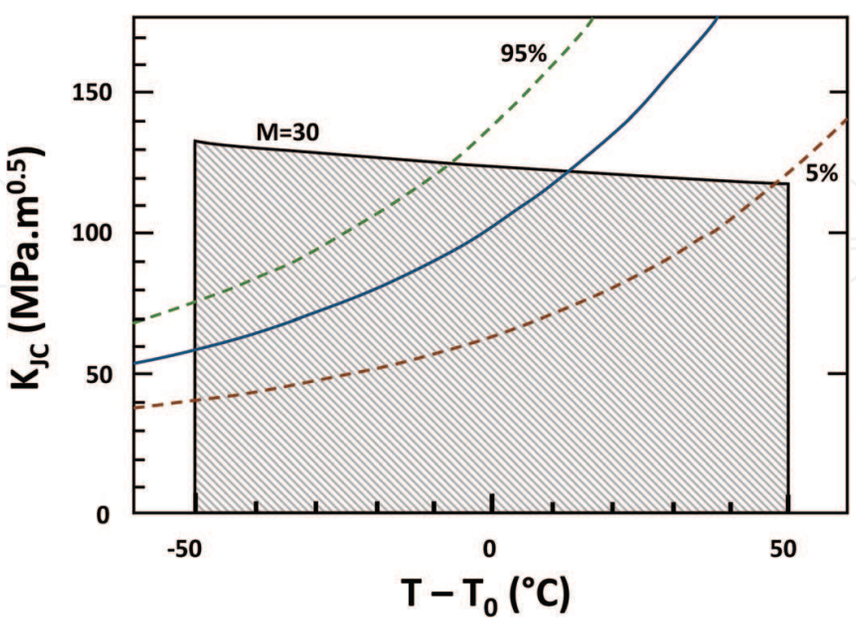

Figure 3. Validity window of the Master Curves for the ferritic materials [6].

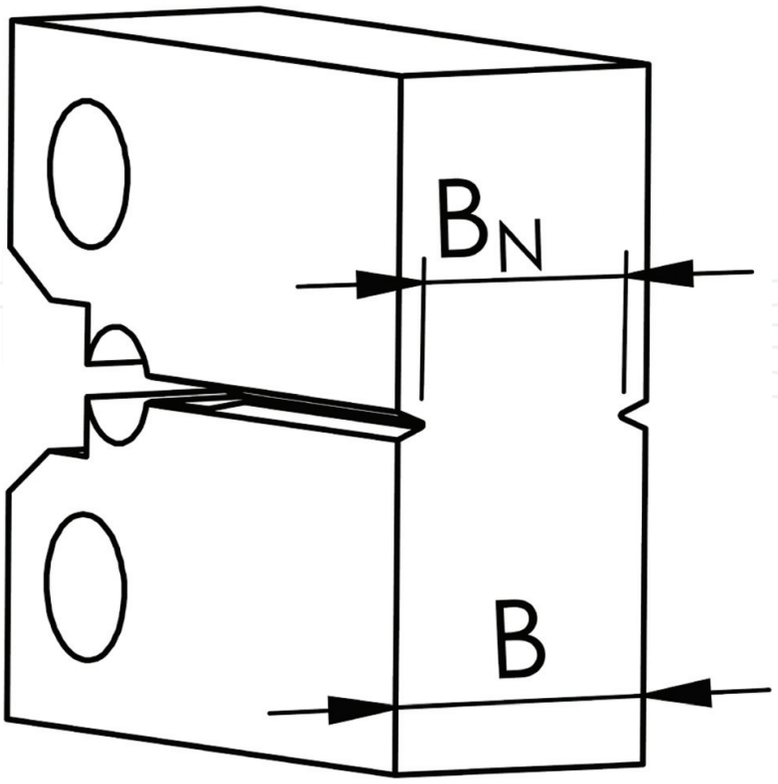

Figure 4. Side grooves in a fracture mechanics test specimen.

Recently, great attention is focused on mini-CT (0.16 T-CT) specimen geometry that can be made out of the broken halves of standard Charpy specimens. In 2014, round robin program focused on verification of the reliability and robustness of experimental data of the mini-CT was carried out among different laboratories. The results of the round robin confirmed that the mini-CT specimens offer a very attractive opportunity to derive the same fracture toughness reference temperature values, T_0, as those derived by larger fracture toughness specimens [12].

Sokolov [13, 14] tested in 2016 and 2017 the mini-CT specimens with dimension of $10 \times 10 \times 4$ mm^3 (see **Figure 5**) on materials HSST Plate 13B and un-irradiated Linde 80 WF-70 weld, respectively. The T_0 value derived from a relatively small number of mini-CT specimens in these studies is in remarkable agreement with the T_0 value previously reported from a much larger number of conventional fracture toughness specimens. At the same time, these studies indicate that in the real practice, it is highly advisable to use much larger number of specimens than the minimum amount prescribed in ASTM E1921, when mini specimens are employed.

Also Wallin in work [15] focused his attention on mini-CT specimen. His work indicates that miniature C(T) specimens fulfilling the ASTM E1921 size requirement behave like larger specimens loaded to the same proportional loading. Side grooving was found to have a minor effect on the initiator locations and was not significantly affected by the side groove geometry.

For completeness, it should be noted that three different methods to quantify constraint have also been proposed, *J* small scale yielding correction, *Q*-parameter and the *T*-stress. [16]. Also Wallin considers *Q*-parameter and the *T*-stress for Master Curve reference temperature T_0

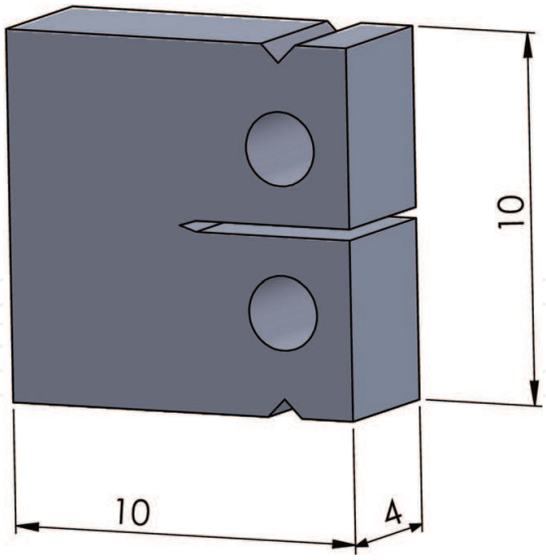

Figure 5. Layout of mini-0.16 T-CT specimens that can be extracted out of the broken halves of Charpy specimens and its overall dimensions.

correction [15, 17]. However closer description of these approaches is out of the scope of the current chapter.

2.3. Ductile region

In the case of ductile materials, first the blunting of preexisting cracks occurs during loading followed by formation of voids ahead of the crack tip at the critical strain. These voids finally coalesce with the crack tip leading to the crack propagation. Hence, the ductile crack initiation cannot be defined as a point in the *J-Δa* curve but rather as a process which occurs over a range. For a *J-R* curve determination, it is necessary to know the crack length at corresponding loading level. There are basically two approaches: single-specimen and multiple specimen methods. For the multiple specimen test method, several "identical" specimens are loaded to different levels, and the achieved crack lengths are usually measured visually at the fracture surface. In the case of the single-specimen method, in order to obtain a full range pf crack lengths for *J-R* curve determination from only one specimen, three widely used single-specimen test methods were developed with the crack lengths being monitored during the test. One is the elastic unloading compliance method that is the most often used out of the single-specimen methods. Another technique is the electrical potential drop method and also the normalization method, both described in the ASTM 1820 [18].

From a *J-R* curve, the characteristic values of elastic-plastic fracture mechanics are determined. One of the significant parameters is the plane strain initiation toughness J_{Ic} that provides a measure of the crack growth resistance near the onset of stable crack growth for mode-I cracks. Since it is difficult to define the instance of crack initiation in ductile metals, different definitions of the initiation toughness were used in different test standards. ASTM E1820 adopts an engineering definition of J_{Ic} at the intersection of a 0.2-mm offset construction line and the *J-R* curve, as shown by J_Q in **Figure 6**.

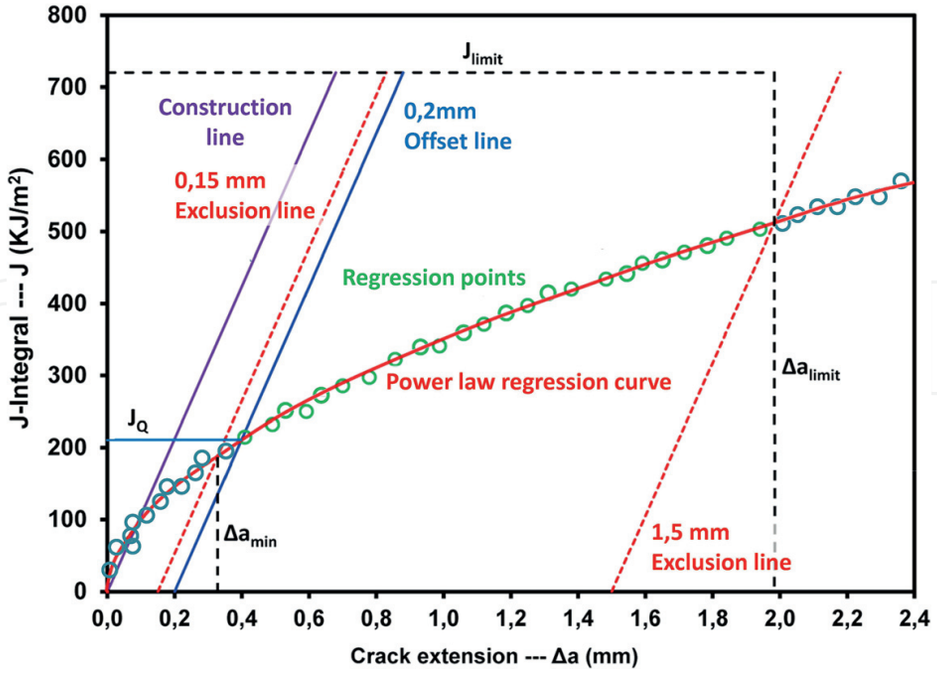

Figure 6. A typical J-R curve with test data points, construction lines and limitation bounds required by ASTM E1820.

A valid J-R curve consists of the measured data points in a region defined by the coordinate axis and the J_{max} and Δa_{max} limits. These two limits describe the measurement capacity of test specimen. The maximum J-integral capacity for a specimen is given by the smaller of:

$$J_{max} = b\sigma_Y/10 \text{ or } J_{max} = B\sigma_Y/10 \tag{5}$$

where σ_Y is an effective yield strength assumed as the average of the 0.2% offset yield strength σ_{YS} and the ultimate tensile strength σ_{tS}. The maximum crack extension capacity for a specimen was defined as

$$\Delta a_{max} = 0.25\, b_0 \tag{6}$$

where b_0 is the initial crack ligament.

Application of fracture mechanics methods to engineering design and structural integrity assessment requires fracture toughness values to be transferred from the laboratory test to a structural application. Experiments have shown that the crack depth, section thickness, specimen size, crack geometry and loading configuration all can have a strong effect on the fracture toughness measurements (*K, G, J* and *d*). These effects are referred to as "constraint effect." Joyce and Link [19] tested SE(B) specimens with various *a/W* ratios to investigate the constraint effect on *J-R* curves. **Figure 7** shows that significant differences exist between the *J-R* curves for deep and shallow cracks. Similar trend can be observed when only one type of geometry with the same ratio of *a/W* but with different sizes is used.

Ono et al. [20] tested JLF-1 steel using 1 CT, 1/2 CT and 1/4 CT in the upper shelf region. Obtained J-R curve are very illustrative and showed shallow shape with decreasing size; see

Figure 8. Specimen size effects were interpreted here in terms of an increase in the plain stress state region and plastic zone size at the crack tip in the specimen. From the point of specimen thickness effect, this work summarized that the fracture toughness increased as the specimen thickness decreased. From the point of ligament size effect, the fracture toughness decreases when the specimens were miniaturized while keeping the same proportions.

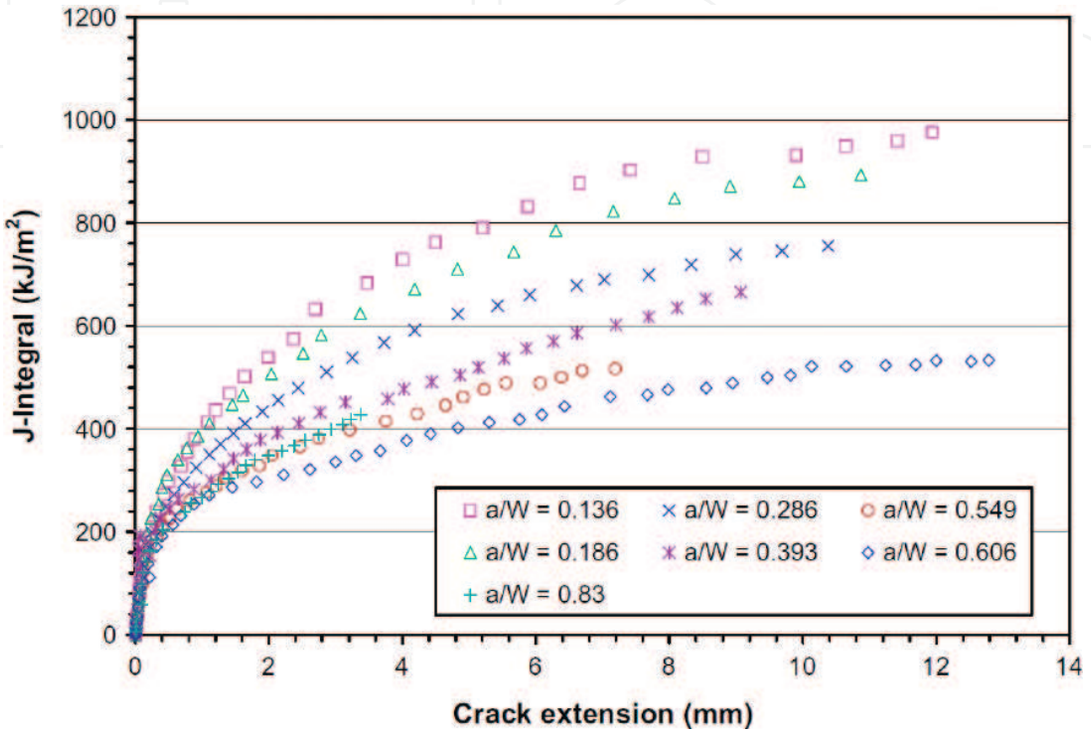

Figure 7. The J-R curve dependency on the a/W ratio for HY80 steel obtained by Zhu and Joyce [19] using SE(B) specimens and normalization method.

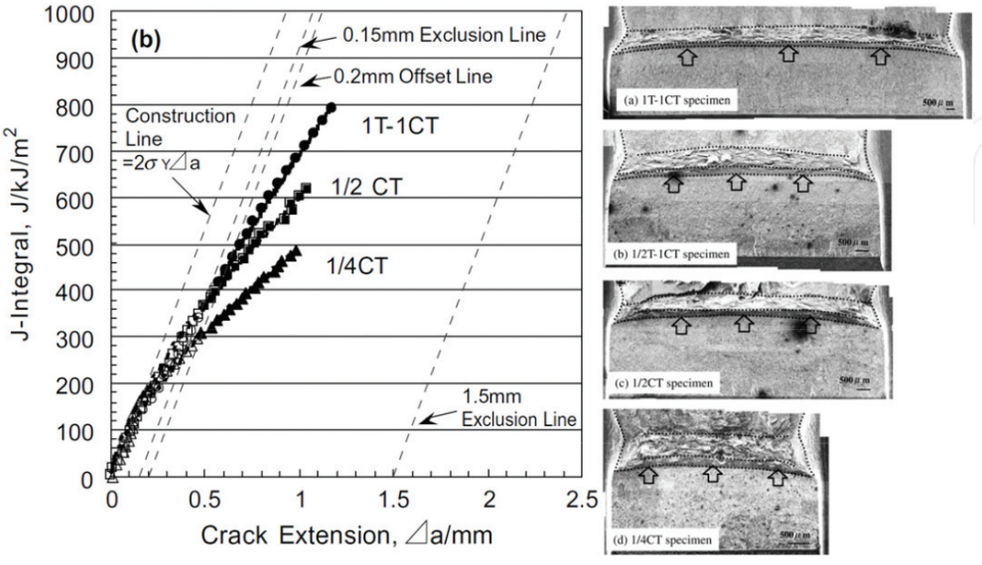

Figure 8. J-R curves of JLF-1 steel (left) and corresponded specimen size (right) [20].

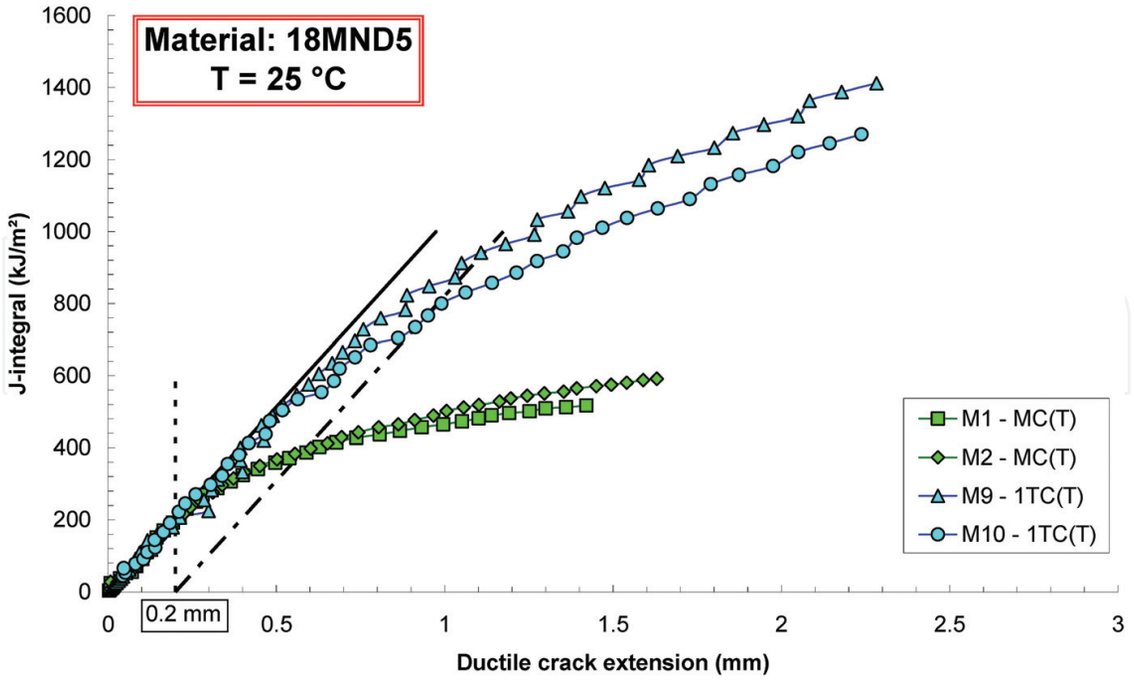

Figure 9. Results obtained at room temperature from mini-CT and 1 T-CT specimens of 18MND5 steel [24].

Seok et al. [21] investigated effect of specimen configurations using 0.5–2 T CT and further specimens with constant width (101.6 mm) but different thickness plus specimens with same thickness but different width. Therefore, the effect of plane size, specimen size and thickness could be investigated. Moreover, the effect of the crack length and side grooves was discussed as well. The resulting *J-R* curve increased with increasing plane size, though there is a difference of increasing amount according to the material states, base or weld metal and stainless or carbon steel. The resulting *J-R* curves decreased with increasing crack length and showed that the effect of the crack length was significant. However, relatively weak influence was observed from the change of the specimen thickness and size. It was also observed that *the J-R* curve decreased by applying the side grooves and the effect of side groove was related to material properties.

Lucon et al. [22–24] investigated mini-CT specimen ($10 \times 10 \times 4.15$ mm^3) applicability for fracture toughness determination in the upper shelf region. As a general conclusion, in these investigations it was observed that mini-CT specimens consistently and systematically underestimate elastic-plastic fracture toughness as measured from 1 T-CT specimens, in terms of both ductile initiation and tearing resistance. **Figure 9** shows an example of such a behavior and also shows that, below approximately J = 200 kJ/m^2, no significant deviation was observed between data measured from mini-CT and 1 T-CT specimen; below this threshold, mini-CT could therefore provide a reliable measurement of the material's toughness.

3. Small size experimental specimen testing

Examples of fracture toughness test with the use of miniature test specimens are going to be presented in this chapter. Results obtained on three experimental materials are shown here.

Namely, RPV steel GOST 15Ch2NMFA with ferritic-martensitic microstructure, austenitic stainless steel EN X5CrNi18-10 (AISI 304) and Ti-Alloy Ti6Al4V produced by Additive Manufacturing (AM) technology are employed in this study. Ductile and brittle materials facture behavior is investigated here with the use of miniaturized specimens applying J-R curve and Master Curve assessment approaches.

As the assessment of the fracture toughness parameters requires also tensile test data as input parameters for the evaluation, determination of tensile properties with the use of miniature tensile test (M-TT) specimens is also demonstrated here.

3.1. Experimental materials

Material GOST 15Ch2NMFA were delivered in a form of rod with diameter of 130 mm and length 150 mm. At first, three 2 T-CT specimens were produced in R-C orientation (according to the standard ASTM E399-09 [3]). Technical drawing of 2 T-CT specimens is depicted in **Figure 10**. Broken halves of the 2 T-CT specimens were subsequently used for production of the other specimens (tensile test specimens, Charpy specimens, etc.).

Material EN X5CrNi18-10 (AISI 304) was delivered in the form of hot rolled rod with quadratic cross section of dimensions 60 × 30 × 400 mm^3. All specimens were produced in T-L orientation according to standard [3].

Material Ti6Al4V was investigated in the form of bar with dimension of 10 × 20 × 100 mm^3. Designation of specimen orientation was done according to the standard [25]. Where the first letter represents the direction normal to the crack plane and second latter represents the expected direction of crack extension. Orientation and its designation of the specimens in the prism are depicted in **Figure 11**.

3.2. Tensile tests

Tensile test were carried out on standard- and miniature-sized specimens at room temperature under quasi-static loading conditions for demonstration of comparable results obtained with the use of miniaturized specimens. Tests were following procedure according to standard (ISO CSN EN 6892-1) in the case of the full-size specimen testing. Testing procedure based on

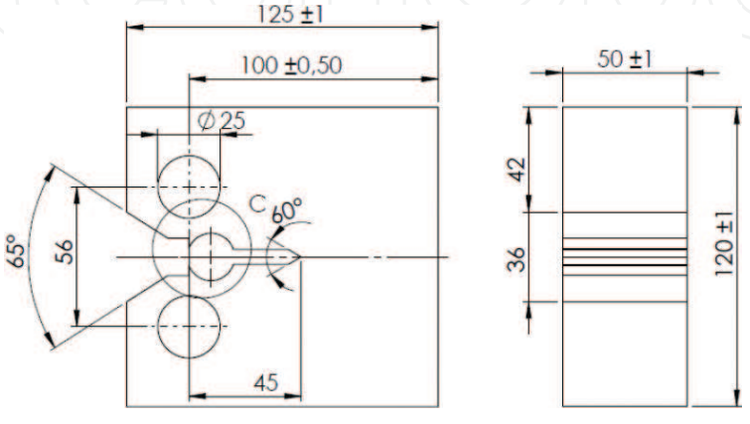

Figure 10. 2 T-CT specimen geometry.

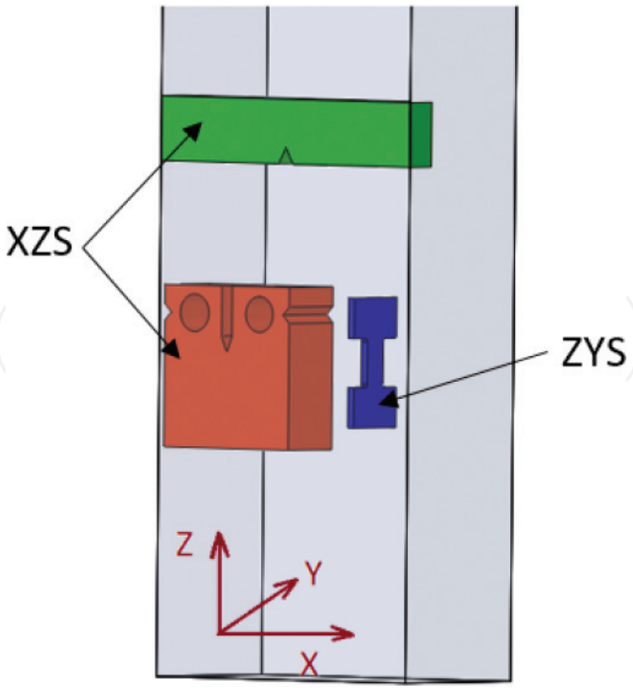

Figure 11. Orientation and designation of the specimens for the material Ti6Al4V produced SLM AM technology (Z = building direction).

standard developed in [26, 27] was employed for mini tensile test (M-TT) specimens. Specimen geometry used for the current investigations is displayed in **Figure 13**. Full size specimens (**Figure 12c**) were tested with the use of electromechanical testing system Zwick Z250 with

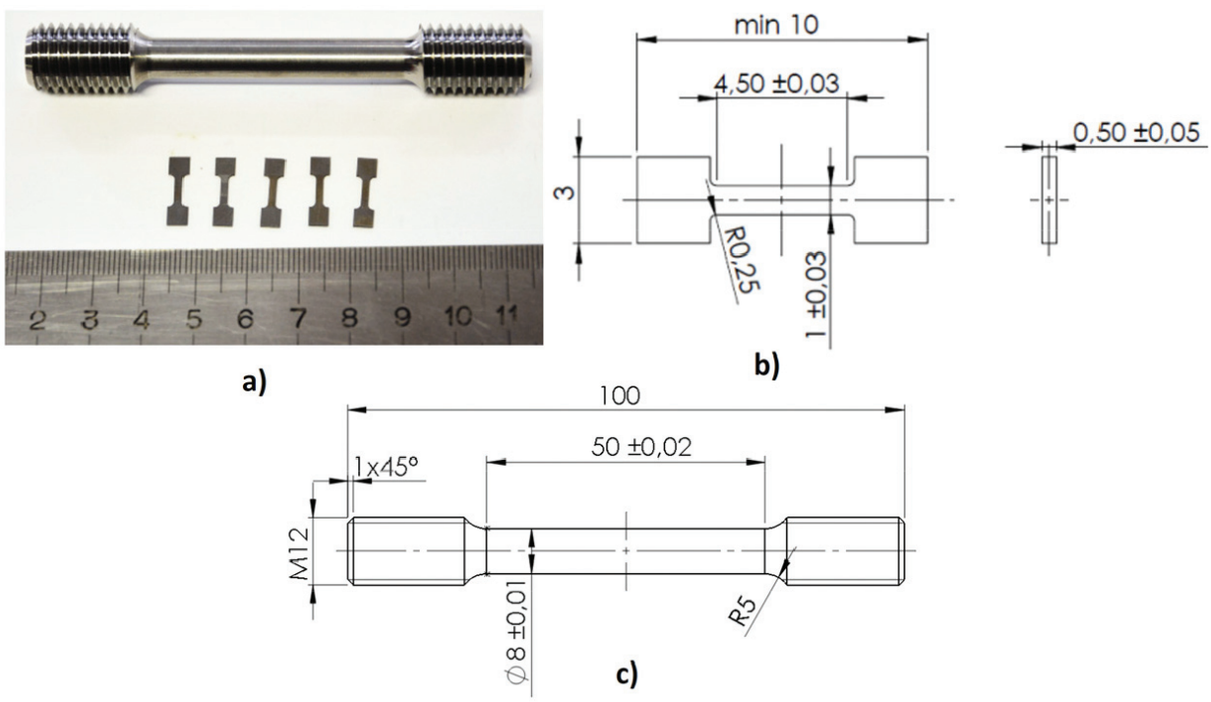

Figure 12. Tensile test specimen geometries. (a) Comparison of the standard and miniature tensile test specimens. (b) Dimensions of mini tensile test (M-TT) specimen. (c) Standard size specimen.

mechanical extensometer for strain measurement. The M-TT specimens (**Figure 12b**) were tested with the use of small-sized linear drive-based testing system with capacity of 5 kN. Strain in the course of the M-TT test was measured using DIC system ARAMIS by GOM. Prior to tests, strain calibration with certified calibration blocks was performed. An appropriate pattern was applied on the specimen surface for the strain measurement by DIC system. M-TTs were done with constant crosshead velocity of 0.25 mm/min and 1 mm/min for the "standard" geometry. Three to five specimens were tested per batch. Specimens' dimensions were measured prior to tests and after tests in order to evaluate tensile test-specific parameters. Summarized test records obtained for the materials investigated are shown in **Figures 13–15**. Averaged test results for each material investigated are shown in **Table 4–6**.

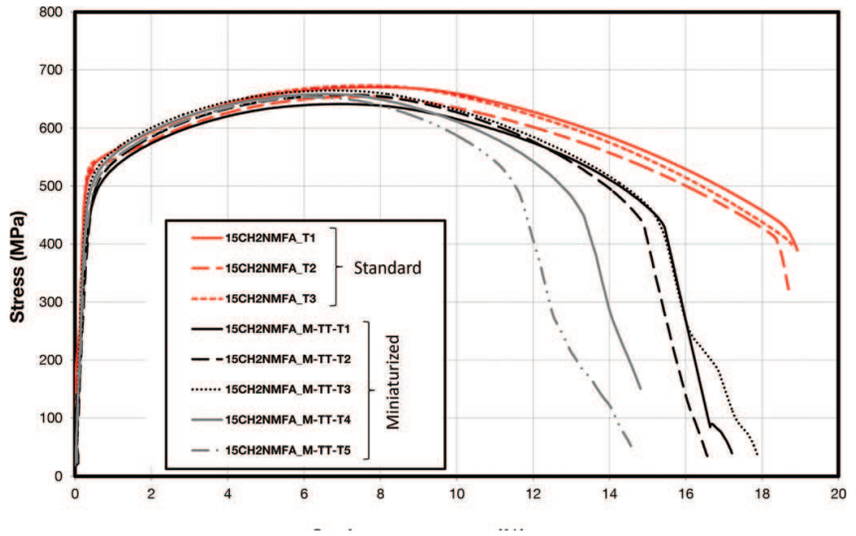

Figure 13. Tensile test results, material 15CH2NMFA, geometry: standard and miniaturized.

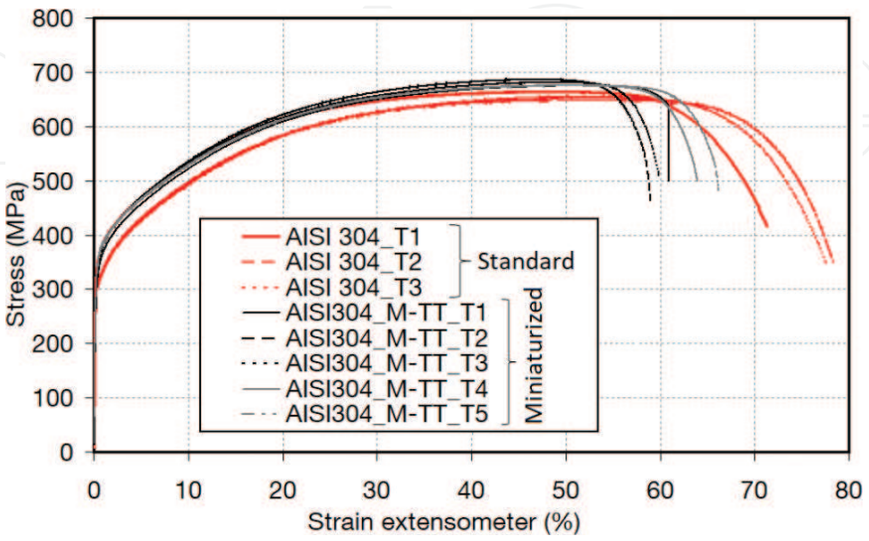

Figure 14. Tensile test results, material AISI304, geometry: standard and miniaturized.

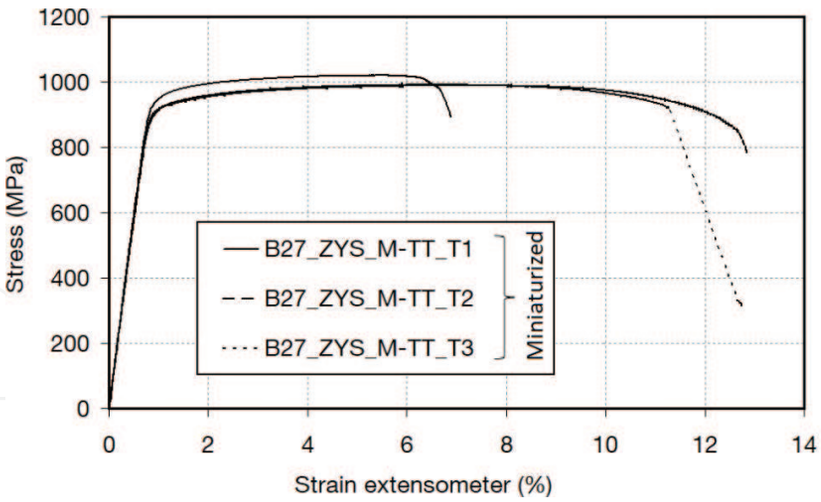

Figure 15. Tensile test results, material AM Ti6Al4V, geometry: M-TT.

Specimen		E	YS	UTS	El_u	El	RA
		GPa	MPa	MPa	%	%	%
AISI304_standard	Avg.	167.6	316.2	657.1	49.1	63.7	82.5
	St. dev.	16.9	27.6	6.8	1.2	2.1	1.8
AISI304_miniaturized	Avg.	141.9	340.7	679.1	49.3	62.0	75.7
	St. dev.	8.1	9.9	4.8	1.3	3.0	1.7

Table 4. Tensile test results, material AISI 304, geometry: standard and miniaturized.

Specimen		E	YS	UTS	El_u	El	RA
		GPa	MPa	MPa	%	%	%
15CH2NMFA_standard	Avg.	195.4	502.0	647.9	8.0	20.8	70.1
	St. dev.	9.5	21.4	13,1	1.1	1.4	0.4
15CH2NMFA_miniaturized	Avg.	159.8	503.4	655,1	6.3	16.2	66.0
	St. dev.	27.9	11.7	8,3	0.3	1.4	5.2

Table 5. Tensile test results, material 15CH2NMFA, geometry: standard and miniaturized.

Specimen		E	YS	UTS	El_u	El	RA
		GPa	MPa	MPa	%	%	%
B27_ZYS_miniaturized	Avg.	114.6	927.3	1000.7	5.5	10.8	43.3
	St. dev.	2.0	20.2	17.1	0.8	3,4	2.1

Table 6. Tensile test results, material AM Ti6Al4V, geometry: miniaturized.

http://dx.doi.org/10.5772/intechopen.73093

3.3. Fracture toughness measurements

Based on theoretical and experimental analyses of possible fracture toughness specimen downsizing, several geometries were proposed as it was discussed before. Demonstration of the fracture toughness property measurement with the use of miniaturize specimens is shown here on samples of several geometries here. The geometries employed here are miniature compact tension specimen (0.16 T-CT) (**Figure 16**) and miniature Charpy specimens (half Charpy specimen typically 4 × 3 × 22, KLST); see **Figure 17**. These specimens' geometries are utilized for brittle and ductile fracture description.

As the input data for the fracture toughness tests are used, results of tensile tests for pre-cracking parameter determination and subsequent evaluation of validity limits and J-R curves.

The effect of the temperature on fracture toughness is known for many years. It is a question of the material if it will exhibit sharp or gentle change. As it was mentioned above, the fracture toughness-temperature dependency can be divided in several regions, and the current tests are covering most of them.

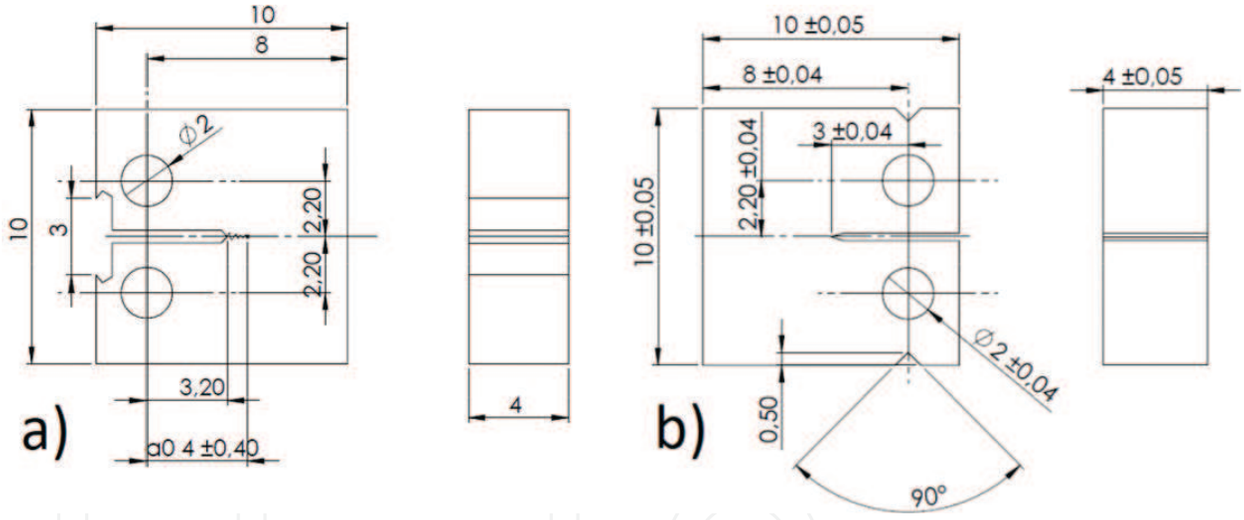

Figure 16. Miniature compact tension specimen (0.16 T-CT): (a) front face geometry and (b) the "top and bottom" geometry.

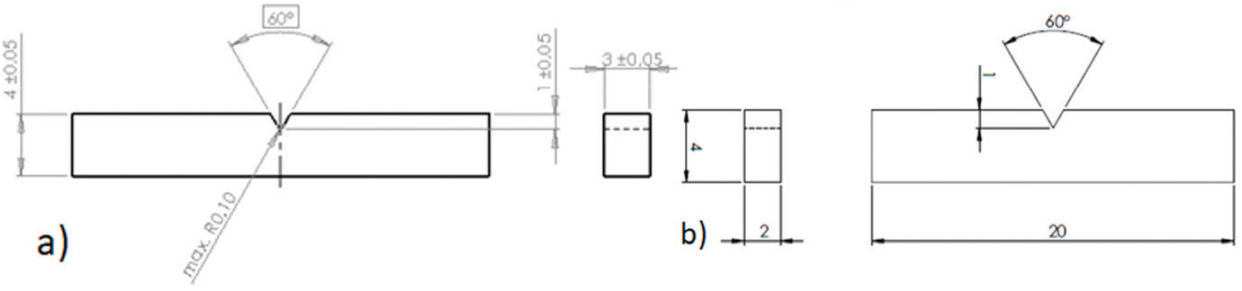

Figure 17. Miniature Charpy specimen (KLST): (a) geometry 4 × 3 × 22 mm^3 and (b) geometry 4 × 2 × 20 mm^3.

3.4. Testing in the transition region

Master Curve concept according to the standard ASTM 1921-17a [5] was applied on material 15CH2NMFA. The aim of this investigation was to show the shift of the reference temperature T_0 with regard to the geometry of the specimen and size of the specimen. Therefore, compact tension specimens of different sizes (2 T-CT, 1 T-CT and 0.16 T-CT) and three-point bend specimens' geometries (CVN, standard Charpy specimen $10 \times 10 \times 55$ mm^3, and miniaturized Charpy specimen, KLST ($3 \times 4 \times 22$ mm^3)) were produced.

Pre-crack of all specimens was done on magnetic resonance testing machine RUMUL; the initial crack size was 0.5 W with the final stress intensity factor of 16 MPa.m$^{0.5}$. After pre-cracking, 20% side groves were introduced. The final tests were performed on servo-hydraulic testing machine MTS 810 with load capacity of 250 kN (in a case of 2 T-CT and 1 T-CT specimens) and servo-hydraulic testing machine Instron with load capacity 80 kN (in a case of CVN, KLST specimens), respectively. Both machines were equipped with environmental chamber for cooling of the specimens. In all cases specimens were held on testing temperature for 15 min before the tests. Deformation of the specimens was measured by means of COD extensometer on the load-line position. Testing setup for KLST samples is depicted in **Figure 18**.

The first estimation of the T_0 was done according to the (7) presented in [5]. For this purpose ten standard Charpy specimens were produced, and value $TK_{28J} = -34.7$ J was determined. The estimated reference temperature T_0 was evaluated according to the (7) as −52.7°C. This estimation provides reference temperature with standard deviation of 15°C [5]:

$$T_0 = TK_{28J} - 18^{\circ}C \tag{7}$$

For measurement and calculation of reference temperature T_0, the multi-temperature approach was applied. All measured data were censored through crack front criterion defined in (8):

$$K_{Jc(limit)} = \sqrt{\frac{Eb_0\sigma_{YS}}{30(1-v^2)}} \tag{8}$$

where E is Young modulus, $b_0 = W\text{-}a_0$ (a_0 = initial crack size), σ_{YS} is yield strength and v is Poisson ratio. For the final evaluation, all fracture toughness results were recalculated to K_{JC_1T} using Eq. (3).

Measured data which fulfill the limit stated in (8) were marked as $r_i = 1$. If evaluated facture toughness values exceed limit (8) value, they were marked as $r_i = 0$, respectively.

Crack lengths were measured through area measurement method. Example of fracture area measurement is presented in **Figure 19**.

Summarization of the reference temperature T_0 determination is shown in **Table 7**. Master Curve with all measured data is depicted in **Figure 20**.

It is clear from **Table 7** that evaluated reference temperature using the KLST specimens and 2 T-CT specimens does not fulfill the validity criteria $\sum r_i n_i > 1$, and these reference temperatures can be taken as provisional reference temperature T_{0Q}.

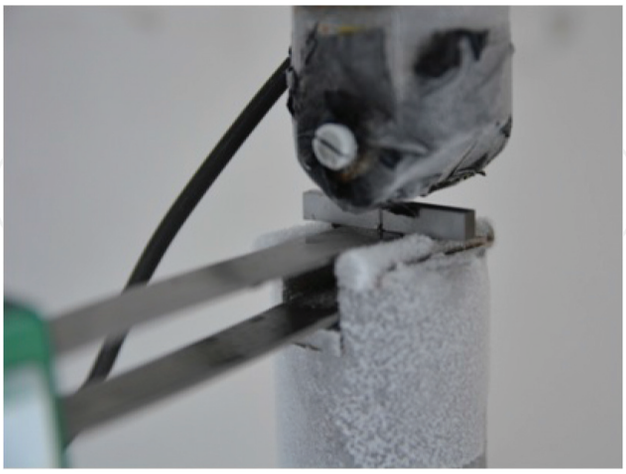

Figure 18. KLST specimens ($4 \times 3 \times 22$ mm^3) from material 15CH2NMFA.

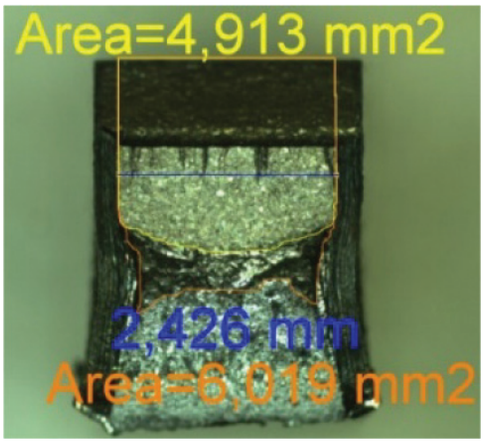

Figure 19. Example of crack size measurement.

Specimen	**Number of specimen**	**T_0/T_{0q}**	**$r_i.n_i$**	**Diff.T_0**
		°C	—	°C
1 T-CT	6	−41,3	1	−23,7
0.16 T-CT	9	−62,6	1,5	−2,4
CVN	14	−73,1	2,33	8,1
KLST	14	−51,8	0,56	−13,2
2 T-CT	3	−27,9	0,5	−37,1
All specimens	46	**−65,0**	**5,9**	—

Table 7. Summarization of Master Curve results, material 15CH2NMFA.

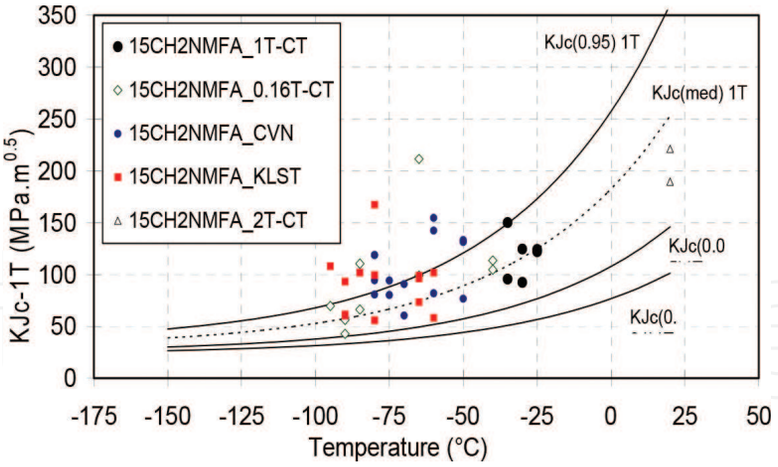

Figure 20. Comparison of the Master Curve evaluation for various samples' geometries.

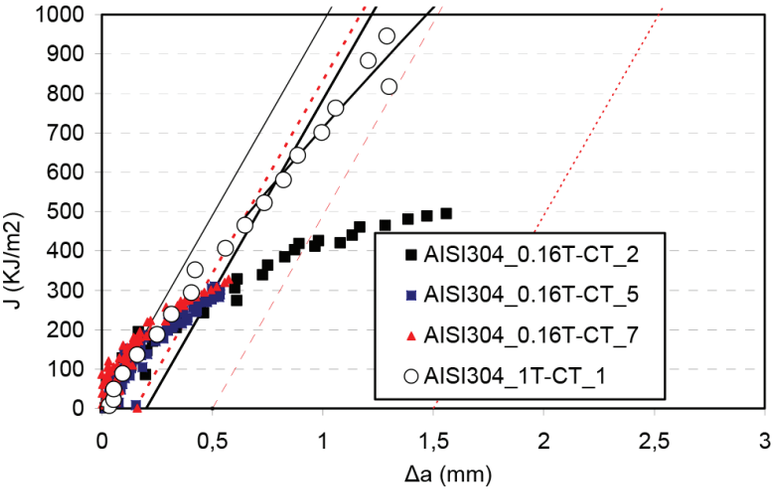

Figure 21. Comparison of J-R curves; material AISI 304; geometry of the specimens, 1 T-CT vs. 0.16 T-CT; unloading compliance method of measurement.

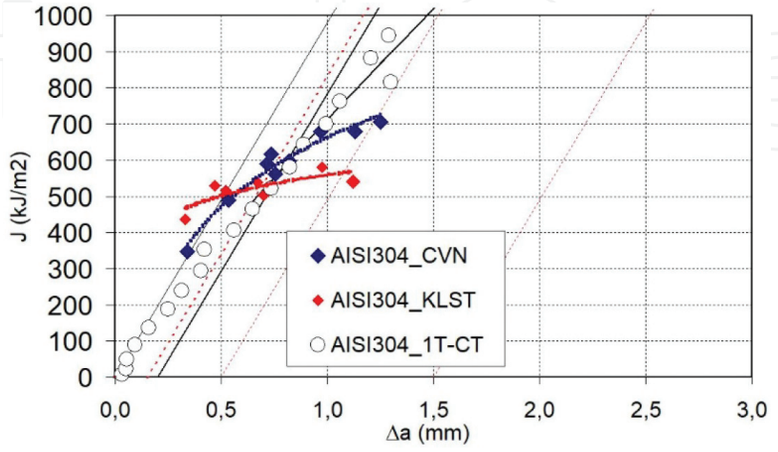

Figure 22. Comparison of J-R curves, material AISI 304, geometry of the specimens: 1 T-CT (unloading compliance method) vs. CVN and KLST (multiple specimen method).

3.5. Testing in the ductile region

Testing in ductile region was done according the standard ASTM 1820-17 [18] where concept of J-R curve was applied with in order to evaluate the crack initiation and propagation of material AISI 304 and material Ti6Al4V produced by AM technology. It compared J-R measured using unloading compliance method (for CT specimen) and multiple specimen method (for three-point-bend specimens); simultaneous size of the specimens was taken into the account. Compact tension specimen (1 T-CT and 0.16 T-CT) was compared with standard Charpy specimen (CVN) and miniaturized Charpy specimens (KLST).

Specimens were pre-cracked at first up to the final initial crack size 0.5 W with the final stress intensity factor of 16 MPa.m$^{0.5}$. After the pre-cracking 20% side groves were introduced, and magnetic resonance machine RUMUL was used for pre-cracking. Testing of 1 T-CT was carried out on servo-hydraulic testing machine MTS 810 with load capacity 250 kN. *J-R* curve tests of CVN, KLST and 0.16 T-CT specimens were carried out on servo-hydraulic testing machine Instron with the load capacity of 80 kN. In the scope of the multiple testing procedures, specimens were heat tinted after the tests and consequently cooled down in liquid nitrogen. The cooled specimens were then broken, and crack sizes were measured through area measurement method; see in **Figure 19**. *J-R* curve evaluation was done with the slope of construction line according to (9):

$$J = 2\sigma_{YS}\Delta a \tag{9}$$

Results of the *J-R* testing are present in **Figures 21–23** and summarized in **Table 8**. Summarization of *J-R* curve tests on material Ti6Al4V produced by Additive Manufacturing technology is in **Table 9**. Comparison of J-R curves obtained for 0.16 T–CT and KLST (4 × 2 × 20 mm^3) is depicted in **Figure 23**.

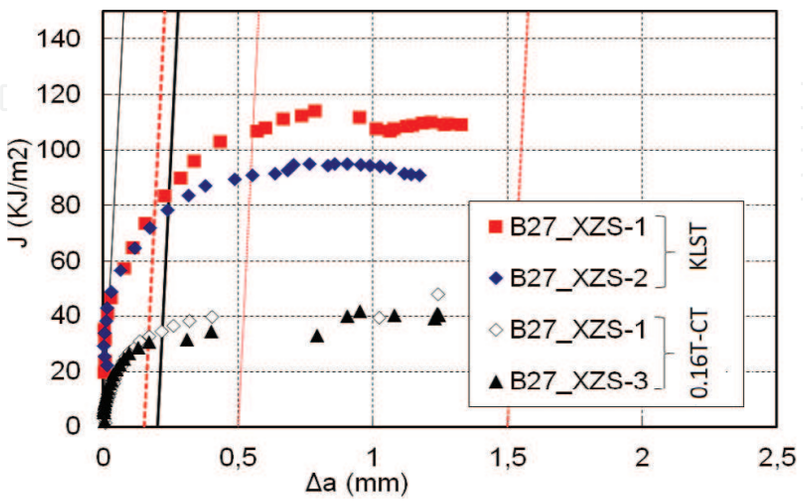

Figure 23. Comparison of J-R curves; material, AM Ti6Al4V; geometry of the specimens, 0.16 T-CT vs. KLST (4 × 2 × 20 mm^3); unloading compliance method of measurement.

Specimen	J_{IC} kJ/m^2	Number of specimens	Specimen
1 T-CT	598,3	3,0	UC
0.16 T-CT	345,2	7,0	UC
CVN	573,1	10,0	MS
KLST	513,6	14,0	MS

(UC = Unloading Compliance; MS = Multiple specimen method)

Table 8. Summarization of average values of fracture toughness results, material AISI 304.

Specimen	O.16 T-CT		KLST (4 × 2 × 20 mm^3)	
	Avg.	St. dev.	Avg.	St. dev.
J_{IC} kJ/m^2	31,9	2,5	85,7	9,1

Table 9. Comparison of fracture toughness results; material AM Ti6Al4V; geometry, 0.16 T-CT vs. KLST (4 × 2 × 20 mm^3); unloading compliance method of measurement.

4. Result discussion and conclusions

The chapter presented here gives basic overview on issues related to small-size specimen testing in the field of the fracture mechanics tests. Some theoretical background and the relation between values obtained on small- and full-sized specimens for all regimes of the fracture behavior ranging from the lower shelf behavior up to the upper shelf region are shown. Some possibilities on how to resolve the size issue influence of the fracture toughness parameters and the reasons for differences obtained during the evaluation in the first chapter part were presented. An overview of size requirements for a valid value determination of the fracture toughness is also given. The subsequent experimental part is demonstrating results of the fracture toughness determination for three materials covering transition and upper shelf region behavior. As an important part of the fracture toughness tests are tensile properties determination. The chapter is dealing with miniature specimen testing; thus mini tensile tests are presented here for the basic property determination that is necessary for fracture toughness test preparation, execution and assessment.

Testing in the transition region and evaluation with the use of the Master Curve approach yielded very good result comparability between miniaturized and full-size specimens for the material investigated. Testing program spanning over five specimens' geometries agrees very well with published results and confirms reliable result determination in this region even with the use of the miniaturized specimens including 4-mm-thick mini-CT specimens and three-point-bend specimens of cross section 2 × 4 mm^2. The upper shelf behavior with the stable crack extension was investigated for stainless steel and Ti-alloy produced by the additive manufacturing process. In the case of the stainless steel, four specimens' geometries were

investigated, and multiple specimens' as well as single specimens' approaches were applied. Standard-sized specimen results yielded very good agreement with the results achieved for subsized three-point bend specimens, while the mini-CT specimen yielded values of about 60% of those ones obtained for standard-sized specimens. In the case of Ti-alloy, due to very limited amount of the experimental material, typically, e.g., for AM parts, mini specimens were investigated only. Both considered specimens' geometries yielded repeatable results. However, the CT specimens yielded significantly lower fracture toughness values of about 40% of those obtained for three-point-bend specimens. Large difference between these specimens' geometries results is in agreement with other published studies and results presented here for the stainless steel.

The results obtained here point out the fact that there is currently no available general solution for size effect description in the fracture toughness determination approaches so far. Varying agreement is found for various materials. Therefore, for a reliable "size-independent" value determination, the material of the interest has to be investigated and size effect quantified. It seems that the *J*-integral-based assessment has rather limited reporting value and better description has to be established for size-independent fracture toughness evaluation in the upper shelf. Lower transition region is well described by the Master Curve approach including size effect in the evaluation. Generally considered, there is no need in all cases to obtain size-independent values. These can be the case such as property assessment of the components of small wall thickness, where plain strain condition is in reality not predominant. Cases when local property anisotropy is being evaluated, just ratio among different locations and/or orientations, are considered. Typical examples of the materials produced with small wall thickness exhibiting high ration of property anisotropy are materials and components produced by the additive manufacturing processes. In these cases, there is generally hardly any chance to obtain "size-independent material properties" due to the reason that if produced in different wall thicknesses, different properties are achieved, and thus considered wall thickness has to be directly assessed.

As it can be seen in many cases, no real size-independent values are possible to achieve for the material, and thus small-size techniques are the only way to characterize the properties. These values are related just to the component and the process considered; however, valuable information are provided allowing component design and process optimization. Miniaturized specimen-based techniques for the fracture toughness determination were demonstrated here as a tool providing deeper insight into the material fracture behavior for better understanding of the material behavior in cases when limited amount of the experimental is available.

Acknowledgements

This chapter was created with support of the projects TH02020448S service life assessment with the use of miniaturized test specimens, 2017–2020, and Development of West-Bohemian Centre of Materials and Metallurgy No. LO1412, financed by the MEYS of the Czech Rep.

Author details

Jan Dzugan*, Pavel Konopik and Martin Rund

*Address all correspondence to: jan.dzugan@comtesfht.cz

COMTES FHT a.s., Dobrany, Czech Republic

References

[1] Holzmann M, Vlach B, Man J. R-curves and fracture toughness transition behaviour at static, rapid and impact loading of Cr-Ni-Mo-V reactor pressure vessel steel. International Journal of Pressure Vessels and Piping. 1995:39-47

[2] Holzmann M, Vlach B, Brumovský M. Measurement of fracture toughness transition behaviour of Cr-Ni-Mo-V pressure vessel steel using pre-cracked Charpy specimens. International Journal of Pressure Vessels and Piping. 1999;**76**:591-598

[3] ASTM E399-09. Standard Test Method for Linear-Elastic Plane-Strain Fracture Toughness KIc of Metallic Materials. West Conshohocken, PA: ASTM Int; 2009

[4] Anderson TL. Fracture Mechanics – Fundamentals and Applications. 3rd ed. Boca Raton: CRC Press; 2005

[5] ASTM E1921-17a. Standard Test Method for Determination of Reference Temperature, to, for Ferritic Steels in the Transition Range. West Conshohocken, PA: ASTM International; 2017 www.astm.org

[6] Feilitzen CF, Sattari-Far I. Implementation of the Master Curve method in ProSACC; 2012, ISSN: 2000-0456

[7] Sattari-Far I, Wallin K. Application of Master Curve Methodology for Structural Integrity Assessments of Nuclear Components, October 2005, ISSN 1104-1374

[8] Wallin K. Master curve analysis of ductile to brittle transition region fracture toughness round robin data, The "EURO" fracture toughness curve, VTT manufacturing Technology; 1998, ISNN 1455-0849

[9] Wallin K, Valo M, Planman T, Rintamaa R. Applicability of Smaller than Charpy Specimens for Fracture Toughness Characterization with the VTT Method. Finland: VTT Manufacturing Technology, FIN-02044 VTT (Espoo); 1997

[10] Scibetta M, Lucon E, Walle E. Optimum use of broken Charpy specimens from surveillance programs for the application of the master curve approach. International Journal of Fracture. 2002;**116**:231-244

[11] Kima BJ, Kasadaa R, Kimuraa A, Tanigawab H. Effects of specimen size on fracture toughness of phosphorous added F82H steels. Fusion Engineering and Design. 2011;**86**(9):2403-2408

[12] Sokolov MA. Results of fracture toughness tests for the round robin test program using mini-compact specimens. In Sokolov MA. ORNL report, ORNL/LTR-2014/686; December 2014

[13] Sokolov MA. Development of Mini-Compact Tension Test Method for Determining Fracture Toughness Master Curves for Reactor Pressure Vessel Steels. Materials Science and Technology Division, Oak Ridge National Laboratory; 2017

[14] Sokolov MA, Nanstad RK. The Assessment and Validation of Mini-Compact Tension Test Specimen Geometry. Materials Science and Technology Division, Oak Ridge National Laboratory; 2016

[15] Wallin K, Yamamoto M, Ehrnstén U. Location of initiation sites in fracture toughness testing specimens - the effect of size and side grooves. Proceedings of the ASME 2016 PVP2016, Vancouver, British Columbia, Canada

[16] Nevalainen MJ. The effect of specimen and flaw dimensions on fracture toughness. VTT Publications 314: Espoo. Technical Research Centre of Finland; 1997

[17] Wallin K. Quantifying T_{stress} controlled constraint by the master curve transition temperature T_0. Engineering Fracture Mechanics. 2001;**68**:303-328

[18] ASTM E1820-17. Standard Test Method for Measurement of Fracture Toughness. West Conshohocken, PA: ASTM International; 2017 www.astm.org

[19] Zhu WK, Joyce JA. Review of fracture toughness (G, K, J, CTOD, CTOA) testing and standardization. U.S. Navy Research. Paper 49; 2012

[20] Ono H, Kasada R, Kimura A. Specimen size effects on fracture toughness of JLF-1 reduced-activation ferritic steel. Journal of Nuclear Materials. 2004;**329–333**:1117-1121

[21] Seok CS, Kim SY. Effect of specimen configurations on the fracture resistance curve. Nuclear Engineering and Design. 2002;**214**:47-56

[22] Lucon E, Scibetta M. Miniature compact tension specimens for upper shelf fracture toughness measurements on RPV steels. American Society for Testing and Materials. 2009;**5**:18-31. ASTM STP 1502

[23] Lucon E, Scibetta M, Vandermeulen W. Additional Investigations on the Applicability of Miniature Compact Tension Specimens for Fracture Toughness Measurements in the Upper Shelf Regime; 2005

[24] Lucon E, Scibetta M, Chaouadi R, van Walle E. Use of Miniaturized Compact Tension Specimens for Fracture Toughness Measurements in the Upper Shelf Regime, OPEN REPORT OF THE BELGIAN NUCLEAR RESEARCH CENTRE, SCK.CEN-BLG-1009; April 2005. online: http://publications.sckcen.be/dspace/bitstream/10038/240/1/blg_1009_text.pdf

[25] ASTM WK49229, Standard Guide for Orientation and Location Dependence Mechanical Properties for Metal Additive Manufacturing; 2017. Work in Progress. http://www.astm.org/DATABASE.CART/WORKITEMS/WK49229.htm

[26] Džugan J, Procházka R, Konopík P. Micro -Tensile Test Technique Development and Application to Mechanical Property Determination. In: Sokolov MA, Lucon E, eds. Small Specimen Test Techniques. Vol. 6, STP 1576. pp. 12-29. doi: 10.1520/STP157620140022

[27] Dzugan J, Konopik P, Rund M, Prochazka R. Determination of Local Tensile and Fatigue Properties with the Use of Sub-Sized Specimens, ASME PVP 2015. Vol. 1A. USA: Codes and Standards, Boston, Massachusetts; 2015. ISBN: 978-0-7918-5692-5, Paper No. PVP2015-45958, pp. V01AT01A066; 8 pages. DOI: 10.1115/PVP2015-45958

IntechOpen

IntechOpen